Modeling and Optimization of Mechanical Properties of PA6/NBR/Graphene Nanocomposite Using Central Composite Design

M. R. Nakhaei*[a], G. Naderi[b]

[a] Faculty of Mechanics and Energy, Shahid Beheshti University, Tehran, Iran
[b] Iran Polymer and Petrochemical Institute, Tehran, Iran

PAPER INFO	ABSTRACT
	Thermoplastic elastomer of PA6/NBR reinforced by various nanoparticles have wide application in many industries. The properties of these materials depend on PA6, NBR, and nanoparticle amount and characteristics. In this study, the simultaneous effect of NBR and graphene nanoparticle content on mechanical, thermal properties, and morphology of PA6/NBR/Graphene nanocomposites investigated by Central Composite Design (CCD). Thermal properties and morphology of PA6/NBR/Graphene nanocomposites were investigated by Differential Scanning Calorimetry (DSC), X-Ray Diffraction (XRD), and Scanning Electron Microscopy (SEM). The results indicate that a small percentage of error between predicted values of mechanical properties and experimental values was achieved. An increase in graphene content have a positive impact on the tensile strength but increasing the NBR phase has the opposite effect. A maximum tensile strength of 35.3 MPa for PA6/NBR/Graphene nanocomposites was obtained at the NBR and graphene content of 20 %wt and 1.5 %wt, respectively. The thermal behavior of the PA6/NBR blend improved with addition graphene. With the addition of 1.5 % graphene content to PA6/NBR blend, the crystallization temperature and melting temperature increased from 192.1 to 196.2 °C and 221.1 to 223.4 °C, respectively. *doi: 10.5829/ije.2020.33.09c.15*

1. INTRODUCTION

Polyamide 6 (PA6) as one of engineering thermoplastics have wide application in various industries such as automobile, aerospace, and shipbuilding due to its chemical and wear resistance, stiffness, excellent strength properties, low friction and high melting points [1, 2]. The properties of PA6 can be enhanced by mixing with fillers and rubber material such as ethylene-propylene-diene monomer (EPDM), poly (epichlorohydrin -co-ethylene oxide) (ECO) and nitrile butadiene rubber (NBR) [3]. Blending PA6 and NBR leads to thermoplastic elastomer (TPE) material with better toughness. In research conducted by Fagundes et al. [3], the mechanical and morphology of PA6/NBR blend (vulcanize and unvulcanize) as influenced by sulfur content was investigated. They concluded that the mechanical performance of PA6/NBR vulcanizes blends

depends on the curing system and morphologies. In addition, the blends of PA6/NBR have good resistance to non-polar solvents. Nakhaei et al. [4] also studied the dynamic crosslinking of PA6/NBR thermoplastic elastomer. The results show that the curing system and dynamic crosslinking in thermoplastic elastomer blends increases the torque which, causes more improvement in mixing. In addition, cured blends have higher tensile strength, elongation, and hardness compared to uncured blends, while cured blends have lower modulus and swelling. The addition of very low content of nanofillers such as nanoclay, carbon nanotube, and graphene enhances mechanical, thermal, and barrier properties dramatically [5, 6]. TPE and TPV nanocomposites are widely consumed in many industries such as automotive, airplane, and ship parts. The effectiveness of nanoparticles such as nanoclay, carbon nanotube, and graphene strongly depends on the uniform dispersion in

*Corresponding Author Institutional Email: *m_nakhaei@sbu.ac.ir*
(M. R. Nakhaei)

the base material [7]. The rheological and morphological properties of PA6/ECO nanocomposites reinforced by 6 % nanoclay was studied by Taghizadeh et al. [8]. They concluded that the increase in ECO content from 0 to 40 % wt increased the melt yield stress from 500 to 22000 Pa. Paran et al. [9] conducted experiments on the PA6/NBR/HNT nanocomposites. The results show that by adding the NBR phase to the PA6 matrix, the impact strength of both unfilled and HNT filled with these materials increased by 22% and 41%, respectively. The crystallization temperature of base material increased with the addition of HNTs, whereas the increase in NBR content decreased this property.

Graphene nanoparticles (2-10nm) consist of many graphene sheets stacked, which, due to platelet morphology, have high tensile strength (130 ± 10 GPa), high aspect ratio (width-to-thickness) and high young's modulus (~1 TPa). This nanoparticle has much application in conductive rubbers and plastics, thermal polymer composites, and also as a filler to improve tensile strength, abrasion resistance, corrosion resistance, stiffness, and lubricant properties [10]. Reviews of previous literature show that many reports on the TPEs nanocomposites, but no studies regarding the effect of graphene on the microstructure, mechanical and thermal properties on PA6/NBR have been reported. In this study, the mechanical properties of PA6/NBR/Graphene nanocomposites were investigated using Response Surface Methodology (RSM). The central composite design with two factors (NBR and graphene) and five levels was applied for developing a mathematical model that is capable of predicting mechanical properties such as impact strength and tensile strength. Thermal properties and morphology of PA6/NBR/Graphene nanocomposites were investigated by Differential Scanning Calorimetry (DSC), X-Ray Diffraction (XRD), and Scanning Electron Microscopy (SEM). Figure 1 shows the flow chart of the research methodology.

2. MATERIALS AND METHODS

2. 1. Materials　　　The grade name, company, and basic specifications of materials in this study are shown in Table 1.

2. 2. Preparation　　　The experiments were designed based on a two - factor five levels central composite design (CCD) with three replications. The input variable parameters are NBR and graphene content. Table 2 shows the level of input variables with their ranges and notations. The NBR and graphene content was varied between 10 wt% to 50 wt% and 0.1 wt% to 0.5 wt%, respectively. For the preparation of the PA6/NBR blend and their nanocomposites, PA6 granules and graphene
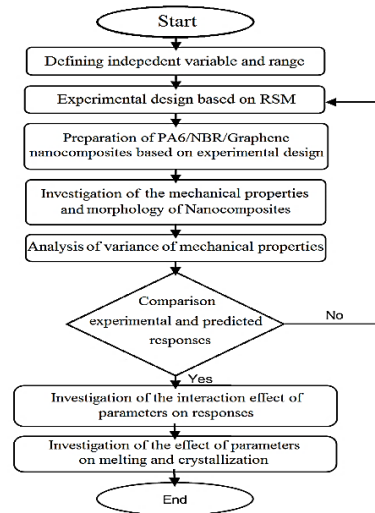

Figure 1. Flow chart of the research methodology

TABLE 1. List of the materials and their characteristics

Material	Company	Grade name	Characteristics
PA6	Kolon plastics (Korea)	KOPA KN136	Density = 1.14 g/cm3 and MFI at 230°C, 2.16 kg = 3.14 g/10 min
NBR	Kumho polychem (Korea)	35L	Mooney viscosity ML (1+8 min) 100 °C = 41 M Acrylonitrile content 34 wt%, Density = 0.98 g/cm3
Graphene	XG Sciences	xGnP-C750	Thickness: 1 - 20 nm, Oxygen content (%): ~10, Lateral size (mm): 1-50, Specific Surface area (m2/g): 750

were dried in a vacuum oven for 24 h and 80 °C. For the preparation of nanocomposites, melt-mixing was performed using an internal mixer (Brabender Plasti-Corder, Germany) with the roller blades, chamber volume 55 cm³, fill factor 0.75, and rotor speed ratio of 2:3. TPO composite with various formulations (according to Table 3) was mixed at 220°C and 80 rpm for 7 min. After melt-mixing the materials, they were dried for about 12 hours at 80 °C in an oven. The suitable samples for mechanical tests and XRD analysis were prepared by the hot press (Collin P 200 E-type) at 230°C for 6 min.

TABLE 2. Parameters, their limits, and levels

Parameters	Notification	Levels				
		-2	-1	0	1	2
NBR (%)	N	10	20	30	40	50
Graphene (%)	G	0	0.5	1	1.5	2

TABLE 3. The formulations of prepared nanocomposites

Code	PA6 (%)	NBR (%)	GPN (%)	Tensile (MPa)	Impact (j/m)
PN0G0	100	0	0	79.0	66
PN30G1	69	30	1	62.5	86
PN40G0.5	59.5	40	0.5	54.2	125
PN50G1	49	50	1	55.1	145
PN30G1	69	30	1	62.4	87
PN30G2	68	30	2	64.0	82
PN30G1	69	30	1	62.7	87
PN30G1	69	30	1	62.4	86
PN30G1	69	30	1	62.6	88
PN30G0	70	30	0	53.3	95
PN20G0.5	79.5	20	0.5	66.1	75
PN40G1.5	58.5	40	1.5	62.3	100
PN10G1	89	10	1	71.0	63
PN20G1.5	78.5	20	1.5	68.5	68

2. 3. Characterization   Impact and tensile strength specimens prepared according to ASTM D256 and D638 type I, respectively [11, 12]. Tensile properties of PA6/NBR/Graphene nanocomposites were performed at a cross-head speed of 1mm/min using a Zuker tensile test machine (Zwhck Co., Germany). The impact strength test was performed in a Zwick 4100 machine. At each experimental condition, which is presented in Table 3, three specimens were tested, and the average of three responses is reported in the same table.

The X-ray diffraction (XRD) of graphene and PA6/NBR nanocomposites was evaluated using a diffractometer (Philips X'Pert PRO, Netherlands) at a scan rate of 1°/min. XRD data were collected using a diffractometer with 50 kV voltage and 40 mA current at room temperature.

The morphology of the specimens was examined using a VEGATESCAN scanning electron microscope. Cryofracture specimens were etched by acetone to extract the NBR phase. The size of the rubber particles was calculated as follows:

$$D_n = \frac{\sum N_i D_i}{\sum N_i} \tag{1}$$

where N_i and D_i are the numbers of particles and their diameters, respectively.

3. RESULTS

3. 1. XRD Analysis   X-ray diffraction (XRD) patterns for graphene and the PN30G1 and PN30G2 nanocomposites illustrated in Figure 2. The diffraction patterns of graphene demonstrate a sharp peak at $2\theta = 25.8°$. According to Bragg's law ($d = \frac{\lambda}{2\sin\theta}$), the interlayer spacing of graphene is 3.45 A. For the PN30G2 and PN30G1 nanocomposite, the peak at 25.8° has shifted to 22.6° (3.93 A) and 18.55° (4.77 A), respectively. The lower angle of PN30G1, and PN30G2 nanocomposite compare to graphene show that the penetration of polymer chain into the graphene layers and better dispersion of graphene in the polymer matrix. For these nanocomposites, it can be seen the significant decrease in peak intensity. The decrease in peak intensity attributed to the exfoliation of graphene layers [12, 13]. This result is consistent with the previous study on PP/EPDM/graphene and elastomer/graphene nanocomposites [10, 13].

3. 2. Analysis of Variance (ANOVA) of Responses
The objective of ANOVA is to determine the significance of model and process parameters in the factorial design technique. In RSM methods, Fisher's variance ratio (F-value) is the measure of variation in the data about the mean and estimated by the sum of square data (SS) [14, 15]. The highest F-value reveals a more signicant effect of the parameters on responses. The Design-Expert V7 Software was used to determining the best regression models that fits experimental data. The results of ANOVA tables of three responses (tables 4-6) show that the NBR was the most significant parameter affecting the tensile strength and impact strength of PA6/NBR/graphene nano-composites. According to ANOVA tables, when the P-value for molds is less than 0.05 (for 95% confidence level), it indicates that the parameters or model terms are significant on the response [14]. According to the theory of ANOVA and ANOVA tables for tensile strength and impact strength, it is seen that linear effects of NBR (N) and graphene (G) content and also the interaction effects of NBR and graphene (N×G) are significant for three responses. The quadratic effect of NBR (N^2) is significant on impact strength,
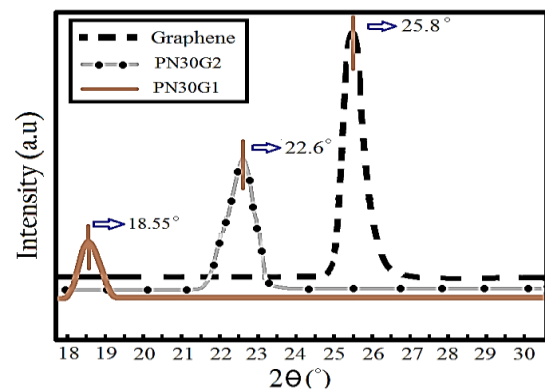

Figure 2. XRD curves of graphene, PN30G2, and PN30G1 nanocomposite

whereas the quadratic effect of graphene (G^2) is significant on tensile strength. In addition, the R^2, adjusted R^2, and predicted R^2 are shown these tables. It can be seen, in all the three responses, that the R^2 values are in reasonable agreement and are close to 1, which is desirable. The high values of adjusted R^2 and predicted R^2 in Tables 4 and 5 shows that the regression models have the great predictive ability.

TABLE 4. ANOVA for the tensile strength

Source	Sum of Squares	df	Mean Square	F-Value	p-value
Model	334.84	5	66.96	121.59	< 0.0001
NBR (N)	212.15	1	212.15	358.89	< 0.0001
Graphene (G)	88.02	1	88.02	159.83	< 0.0001
N×G	7.56	1	7.56	13.73	0.0076
G^2	22.36	1	22.36	40.61	0.0004
N^2	0.43	1	0.43	0.78	0.4060
Residual	3.86	7	0.55		
Lack of Fit	3.79	3	1.26	1.21	0.5703
R^2	0.989		Adj R^2		0.981
Pred R^2	0.913		Adeq Precision		36.37

TABLE 5. ANOVA for the Impact strength

Source	Sum of Squares	df	Mean Square	F-Value	P-value
Model	6416.39	5	1283.28	108.44	< 0.0001
NBR (N)	5808.01	1	5808.01	490.78	0.0018
Graphene (G)	280.33	1	280.33	23.69	< 0.0001
N×G	81.05	1	81.05	6.84	0.0010
G^2	5.83	1	5.83	0.49	0.5055
N^2	242.67	1	242.67	20.51	0.0286
Residual	82.84	7	11.83		
Lack of Fit	81.64	3	27.21	90.71	0.6628
R^2	0.983		Adj R^2		0.978
Pred R^2	0.876		Adeq Precision		37.65

From the discussion above, the final mathematical models to estimate tensile strength and impact strength of nanocomposites are represented in Equations (2) and (3).
In terms of actual factors

$$Tensile\ strength = 45.53 + 5.07 \times G - 0.778 \times N + 0.275 \times G \times N - 3.951 \times G^2 \quad (2)$$

$$Impact\ strength = 35.04 + 13.298 \times G + 1.147 \times N - 0.9 \times G \times N + 0.032 \times N^2 \quad (3)$$

3. 3. Confirmation Experiments To investigate the validity of the developed models, three confirmation experiments were performed under new test conditions. The experimental condition, the actual values of three responses, the predicted values, and the percentages of error are shown in Table 6. Based on Table 6, data corresponding to the confirmation experiments is in good agreement with experimental values [16].

3. 4. The Interaction Effect of Parameters on Mechanical Properties Figure 3 (a and b) is a perturbation plot that illustrates the main effects plot of NBR (N) and graphene (G) for tensile strength and impact strength of nanocomposites, respectively. With increasing graphene content, the tensile strength

TABLE 6. Comparison of actual and predicted responses

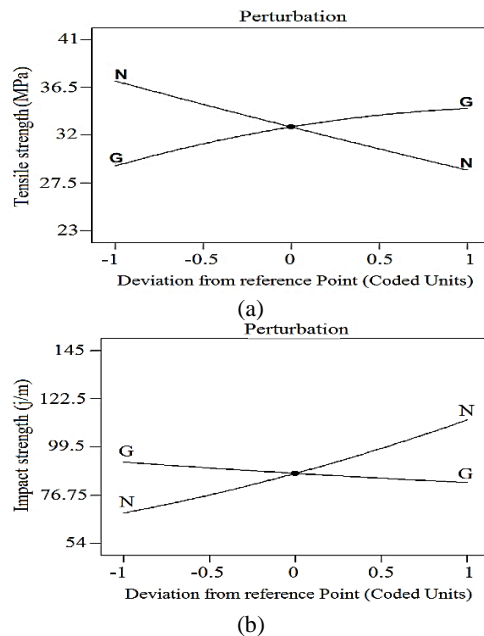| N	G	Tensile strength		Impact strength	
		Actual	70.5	Actual	74.1
20	1	Predict	67.1	Predict	70.2
		Error (%)	5.1	Error (%)	5.5
		Actual	63.9	Actual	95.2
30	0.5	Predict	59.3	Predict	91.6
		Error (%)	7.7	Error (%)	3.9
		Actual	55.8	Actual	105.5
40	1	Predict	58.6	Predict	111.1
		Error (%)	4.7	Error (%)	5.1

Figure 3. Perturbation plots showing the effect of all factors on (a) Tensile strength (b) Impact strength

increased while the impact strength of PA6/NBR nanocomposites reduces slightly with increasing the graphene content. The enhancing effect of graphene (G) on the tensile strength of PA6-based nanocomposites was also reported in other papers [17]. From Figure 3, it can also be observed that the tensile strength of nanocomposites decreased with an increase in NBR phase content which is related to the lower tensile strength of neat NBR, whereas increasing the HNT from 20 to 40 wt% leads to an increase in the impact strength from about 65 to 110 j/m. This phenomenon has also been reported in numerous other PP/elastomer nanocomposites and is due to the softening effect of an elastomeric phase like NBR on plastic-based nanocomposites [17, 18].

Figures 4 and 5 show the 3D response surface plots created by the applied software. The interaction effect between NBR and Graphene content on the tensile strength and impact strength are presented in Figures 4 and 5, respectively. Figure 4 (a and b) show that at low NBR content, the maximum tensile strength of the PA6/NBR/Graphene nanocomposites was obtained at the graphene content of 1.5%. This is related to the fact that the higher nanoparticle content in thermoplastic elastomers leads to decreased size of elastomer particles and consequently, an improvement in the mechanical properties. Haghnegahdar et al. [10] concluded that higher contents of nanographene decrease the size of the dispersed phase.

The average size of rubber particles of prepared PA6/NBR/Graphene nanocomposites was reported in Table 7. Figure 6 shows the cryofractured surfaces of PN30G0, and PN30G2 samples, and the dark holes represent the NBR phase by selectively etching in acetone. Comparing the two samples shows that very small rubber particles are obtained when using 2 %wt of graphene nanoparticle. According to Equation (1) and Figure 6, the size of the NBR phase was decreased from 3.24 to 0.85 µm with the addition of 2 %wt of graphene. Paran et al. [9] concluded that higher contents of halloysite nanotube decrease the size of the NBR phase in the PA6 matrix. They stated that this might be because the viscosity difference between matrix and rubber decreases by adding HNTs to PA6/NBR. The results of research by Haghnegahdar et al. [19] show that another possible effect may be the hindering role of graphene on the coalescence of rubber particles.

The best impact strength of the PA6/NBR/Graphene nanocomposite (122.25 j/m) is achieved at 40 wt% of NBR content and 0.5 wt% of graphene content, according to Figure 5. According to Figure 5, at the minimum amount of loading of NBR, the effect of graphene content on impact strength was not much. With the addition of nanoparticles to PA6/NBR, the size of elastomer decreased, which this behavior increases impact strength. On the other hand, nanoparticles act as stress

concentration which leads to decreases impact strength. Previous results by some other researchers shows that the different effect of nanoparticles on the microstructure of thermoplastic elastomer is the reason for not changing the value of impact strength at a low level of NBR content [9, 11].
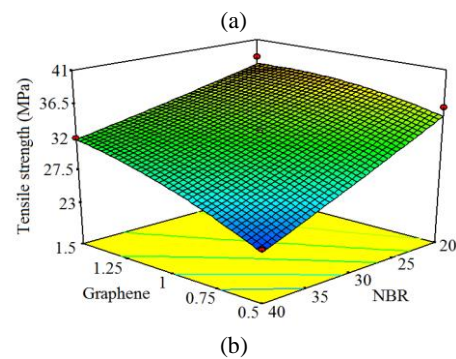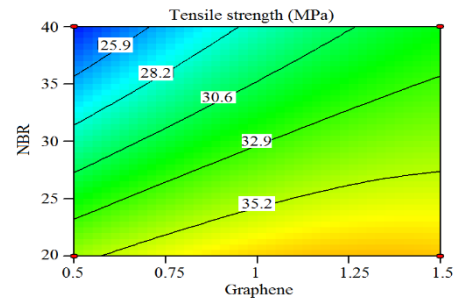
Figure 4. (a) Contours plots and (b) response surface diagram showing the effect of N and G on tensile strength
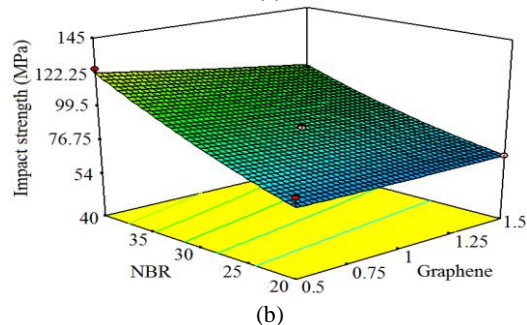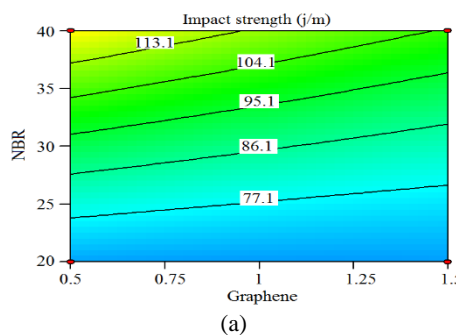
Figure 5. (a) Contours plots and (b) response surface diagram showing the effect of N and G on impact strength
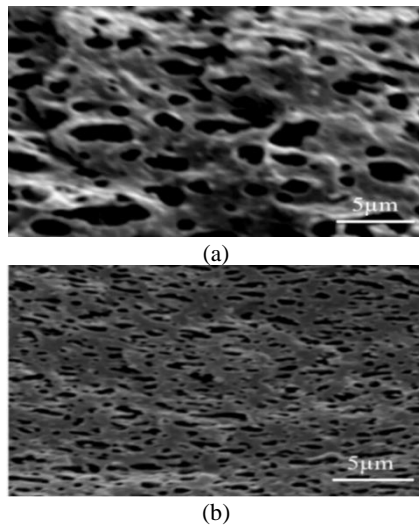
(a)

(b)

Figure 6. SEM micrograph of PA6/NBR/Graphene blend with (a) 0% (b) 2% Graphene content

TABLE 7. Rubber particle sizes of PA6/NBR nanocomposites prepared with graphene

	PN30G1	PN40G0.5	PN50G1	PN30G2
Rubber size (μm)	2.12	4.35	4.93	0.85
	PN30G0	**PN20G0.5**	**PN40G1.5**	**PN20G1.5**
	3.24	1.98	2.87	1.03

At the high level of NBR content, impact strength decreased with an increase in graphene content at 0.5 to 1.5 wt%. This behavior could be related to the weak compatibility and adhesion between NBR as the dispersed phase and PA6 as the continuous phase, especially at the high content of NBR [19].

The best impact strength of the PA6/NBR/Graphene nanocomposite (122.25 j/m) is achieved at 40 wt% of NBR content and 0.5 wt% of graphene content, according to Figure 5. At the minimum amount of loading of NBR, effect of graphene content on impact strength was not much. The different effect of nanoparticles on the microstructure of thermoplastic elastomer is the reason for not changing the value of impact strength at a low level of NBR content [20].

At the high level of NBR content, impact strength decreased with an increase in graphene content at 0.5 to 1.5 wt%. This behavior could be related to the weak compatibility and adhesion between NBR as the dispersed phase and PA6 as the continuous phase, especially at the high content of NBR [18].

3. 5. Effect of Parameters on Crystallization
Table 8 shows the melting and crystallization properties of PA6/NBR/Graphene nanocomposites. Delta H (ΔH) was obtained by DSC thermograms and the area under

TABLE 8. Melting and crystallization temperatures of PA6/NBR/Graphene nanocomposites

Code	ΔH_m (J/g)	X_c (%)	T_c (°C)	T_m (°C)
PN30G1	44.9	20.1	197.2	222.4
PN40G0.5	46.5	20.2	194.1	221.9
PN50G1	44.8	18.9	194.1	222.0
PN30G2	43.1	19.4	198.7	222.8
PN30G0	47.7	21.4	195.1	221.5
PN20G0.5	47.1	21.1	197.2	222.3
PN40G1.5	43.5	19.1	196.1	222.2
PN10G1	46.4	20.4	199.8	223.0
PN20G1.5	44.6	20.1	199.2	222.8

the peak. The crystallinity percent (χ) of these materials was calculated from Equation (4):

$$\chi \ (\%) \ = \ \frac{\Delta H}{\Delta H_m} \times 100 \qquad (4)$$

According to the results in Table 8, comparing ΔH, crystallinity percent, crystallization temperature and melting temperature of the samples PN30G0 and PN30G2 shows that the addition of graphene nanoparticle to the PA6/NBR blend led to decrease ΔH and crystallinity percent. At the same time, it increases the crystallization temperature and melting temperature. With addition of 2 wt% graphene content to PA6/NBR blend, the crystallization temperature, and melting temperature increased from 195.1 to 198.7 °C and 221.5 to 222.9 °C, respectively. This behavior attributed to the fact that graphene nanoparticles act as a nucleating agent and increase crystallization temperature [10]. The addition of graphene and rubber particles decreased size and increased the number of spherulites of PA6, which this behavior led to decreasing the percentage of crystallinity. According to Table 8, comparing the PN30G0 and PN30G2 and also PN10G1 and PN50G1 shows that the addition of 2% of graphene and 40% rubber content to PA6/NBR blends decreases the percentage of crystallinity from 21.4 to 19.4% and 20.4 to 18.9 %, respectively. These results were attributed to the effect of nanoparticle and rubber on the size of the spherulites of the PA6 matrix that these results consistent with the results of other researchers [19, 20].

4. CONCLUSION

In this study, the response surface methodology was used to examine the effects of NBR and graphene content on responses such as tensile strength and impact strength. Experiments were designed based on central composite design. The most important results are as follows:

1. The interlayer spacing of graphene in the nanocomposite with 1 wt% graphene compare to graphene was increased from 3.45 to 4.77A that this show the better dispersion of graphene in the polymer matrix.

2. The rubber particle size decreased from 3.24 to 0.85 µm when graphene content increased from 0 to 2 wt%.

3. At the high level of NBR content, impact strength decreased from 122.5 j/m to 98.3 j/m with an increase in graphene content at 0.5 to 1.5 wt%, while the tensile strength increased from 23.1 MPa to 32.2 MPa.

4. At low NBR content, the maximum tensile strength (36.5 MPa) and impact strength (76.8 j/m) of the PA6/NBR/Graphene nanocomposites was obtained at the graphene content of 1.5%.

5. The addition of graphene nanoparticle to the PA6/NBR blend led to decrease the crystallinity percent and Delta H.

6. With addition of 2% graphene content to PA6/NBR blend, the crystallization temperature, and melting temperature increased from 195.1 to 198.7 °C and 221.5 to 222.9 °C, respectively.

5. REFERENCES

1. Azdast, T., and Hasanzadeh, R. "Tensile and Morphological Properties of Microcellular Polymeric Nanocomposite Foams Reinforced with Multi-walled Carbon Nanotubes." *International Journal of Engineering, Transactions C: Aspects*, Vol. 31, No. 3, (2018), 504–510. https://doi.org/10.5829/ije.2018.31.03c.14

2. Adejuyigbe, I. B., Chiadighikaobi, P. C., and Okpara, D. A. "Sustainability Comparison for Steel and Basalt Fiber Reinforcement, Landfills, Leachate Reservoirs and Multi-Functional Structure." *Civil Engineering Journal*, Vol. 5, No. 1, (2019), 180. https://doi.org/10.28991/cej-2019-03091235

3. Fagundes, E. C. M., and Jacobi, M. A. M. "TPVs PA/NBR: Sistema de reticulação e propriedades." *Polimeros*, Vol. 22, No. 2, (2012), 206–212. https://doi.org/10.1590/S0104-14282012005000021

4. Nakhaei, M. R., Mostafapour, A., and Naderi, G. "Optimization of mechanical properties of PP/EPDM/ clay nanocomposite fabricated by friction stir processing with response surface methodology and neural networks." *Polymer Composites*, Vol. 38, (2017), E421–E432. https://doi.org/10.1002/pc.23942

5. Nakhaei, M. R., Mostafapour, A., Dubois, C., Naderi, G., and Reza Ghoreishy, M. H. "Study of morphology and mechanical properties of PP/EPDM/clay nanocomposites prepared using twin-screw extruder and friction stir process." *Polymer Composites*, Vol. 40, No. 8, (2019), 3306–3314. https://doi.org/10.1002/pc.25188

6. Mosalman, S., Rashahmadi, S., and Hasanzadeh, R. "The Effect of TiO2 Nanoparticles on Mechanical Properties of Poly Methyl Methacrylate Nanocomposites." *International Journal of Engineering, Transactions B: Applications*, Vol. 30, No. 5, (2017), 807–813. https://doi.org/10.5829/idosi.ije.2017.30.05b.22

7. Mostafapour, A., Naderi, G., and Nakhaei, M. R. "Effect of process parameters on fracture toughness of PP/EPDM/nanoclay nanocomposite fabricated by novel method of heat assisted Friction stir processing." *Polymer Composites*, Vol. 39, No. 7, (2018), 2336–2346. https://doi.org/10.1002/pc.24214

8. Taghizadeh, E., Naderi, G., and Razavi-Nouri, M. "Effects of organoclay on the mechanical properties and microstructure of PA6/ECO blend." *Polymer Testing*, Vol. 30, No. 3, (2011), 327–334. https://doi.org/10.1016/j.polymertesting.2011.01.007

9. Paran, S. M. R., Naderi, G., and Ghoreishy, M. H. R. "Microstructure and mechanical properties of thermoplastic elastomer nanocomposites based on PA6/NBR/HNT." *Polymer Composites*, Vol. 38, (2017), E451–E461. https://doi.org/10.1002/pc.23936

10. Haghnegahdar, M., Naderi, G., and Ghoreishy, M. H. R. "Fracture toughness and deformation mechanism of un-vulcanized and dynamically vulcanized polypropylene/ethylene propylene diene monomer/graphene nanocomposites." *Composites Science and Technology*, Vol. 141, (2017), 83–98. https://doi.org/10.1016/j.compscitech.2017.01.015

11. Nakhaei, M., Bani Mostafa Arab, N., and Rezaei, G. "Investigation on Tensile Strength of Friction Stir Welded Joints in PP/EPDM/Clay Nanocomposites." *International Journal of Engineering, Transactions C: Aspects*, Vol. 28, No. 9, (2015), 1383–1391. https://doi.org/10.5829/idosi.ije.2015.28.09c.17

12. Bakhtiari, A., Ashenai Ghasemi, F., Naderi, G., and Nakhaei, M. R. "An approach to the optimization of mechanical properties of polypropylene/nitrile butadiene rubber/halloysite nanotube/polypropylene- <scp> g </scp> -maleic anhydride nanocomposites using response surface methodology." *Polymer Composites*, Vol. 41, No. 6, (2020), 2330–2343. https://doi.org/10.1002/pc.25541

13. Berki, P., László, K., Tung, N. T., and Karger-Kocsis, J. "Natural rubber/graphene oxide nanocomposites via melt and latex compounding: Comparison at very low graphene oxide content." *Journal of Reinforced Plastics and Composites*, Vol. 36, No. 11, (2017), 808–817. https://doi.org/10.1177/0731684417690929

14. Feng, X., Tufail, R. F., and Zahid, M. "Experimental Investigation and Statistical Modeling of FRP Confined RuC Using Response Surface Methodology." *Civil Engineering Journal*, Vol. 5, No. 2, (2019), 268. https://doi.org/10.28991/cej-2019-03091243

15. Moradi, H. M., Zinatizadeh, A. A., and Zinadini, S. "Influence of Operating Variables on Performance of Nanofiltration Membrane for Dye Removal from Synthetic Wastewater Using Response Surface Methodology." *International Journal of Engineering, Transactions C: Aspects*, Vol. 29, No. 12, (2016), 1650–1658. https://doi.org/10.5829/idosi.ije.2016.29.12c.03

16. Mostafapour, A., Akbari, A., and Nakhaei, M. R. "Application of response surface methodology for optimization of pulsating blank holder parameters in deep drawing process of Al 1050 rectangular parts." *International Journal of Advanced Manufacturing Technology*, Vol. 91, No. 1–4, (2017), 731–737. https://doi.org/10.1007/s00170-016-9781-z

17. Tarawneh, M. A., Yu, L.-J., Al-Tarawni, M. A., and Ahmad, S. "High performance thermoplastic elastomer (TPE) nanocomposite based on graphene nanoplates (GNPs)." *World Journal of Engineering*, Vol. 12, No. 5, (2015), 437–442. https://doi.org/10.1260/1708-5284.12.5.437

18. Asgarzadeh, Z., and Naderi, G. "Morphology and properties of unvulcanized and dynamically vulcanized PVC/NBR blend reinforced by graphene nanoplatelets." *International Polymer Processing*, Vol. 33, No. 4, (2018), 497–505. https://doi.org/10.3139/217.3515

19. Haghnegahdar, M., Naderi, G., and Ghoreishy, M. H. R. "Microstructure and mechanical properties of nanocomposite based on polypropylene/ethylene propylene diene monomer/graphene." *International Polymer Processing*, Vol. 32, No. 1, (2017), 72–83. https://doi.org/10.3139/217.3286

20. Hajibaba, A., Naderi, G., Esmizadeh, E., and Ghoreishy, M. H. R. "Morphology and dynamic-mechanical properties of PVC/NBR blends reinforced with two types of nanoparticles." *Journal of Composite Materials*, Vol. 48, No. 2, (2014), 131–141. https://doi.org/10.1177/0021998312469242

Persian Abstract

چکیده

پلاستیک گرمانرم الاستومرهای تقویت شده با نانوذرات مختلف به صورت گسترده در صنایع مختلف کاربرد دارد. در این تحقیق، تاثیر همزمان مقدار گسترده‌ای NBR و درصد نانوذرات بر روی خواص مکانیکی، حرارتی و ریزساختار نانوکامپوزیت‌های PA6/NBR/Graphene با طراحی مرکزی مرکب بررسی شده است. خواص حرارتی و ریز ساختار نانو کامپوزیت ها با استفاده از آزمون گرماسنجی تفاضلی روبشی (DSC)، پراش اشعه ایکس (XRD) و میکروسکوپ الکترونی روبشی (SEM) مورد بررسی قرار گرفت. نتایج نشان می دهد که درصد خطای کوچکی بین نتایج پیش بینی و نتایج تجربی بدست آمده است. افزایش مقدار گرافن تاثیر مثبت بر روی استحکام کششی دارد اما افزایش NBR تاثیر منفی دارد. ماکزیمم استحکام کششی ۳۵/۵ MPa برای PA6/NBR/Graphene هنگامی بدست خواهد آمد که مقدار NBR و گرافن به ترتیب ٪۲۰ و ۱/۵٪ است. رفتار حرارتی کامپوزیت PA6/NBR با افزودن گرافن بهبود خواهد یافت. با افزودن ۱/۵ ٪ گرافن به ترکیب PA6/NBR، دمای بلورینگی و دمای ذوب به ترتیب از ۱۹۲/۱ به ۱۹۶/۲ °C و از ۲۲۱/۱ به ۲۲۳/٤ °C درجه سانتی گراد افزایش یافت